To appear in *Proceedings of SPIE* (1999). Los Alamos National Laboratory document LA-UR-99-3117.

Design and Characterization of Cylindrical CdZnTe Detectors with Coplanar Grids

Thomas H. Prettyman,[*a] Morag K. Smith,[a] and Steven E. Soldner[b]

[a]Los Alamos National Laboratory, MS E540, Los Alamos, NM 87545

[b]eV PRODUCTS, Saxonburg, PA 16056

ABSTRACT

This paper describes the development of cylindrical coplanar grid CdZnTe detectors for gamma ray spectroscopy. Cylindrical detectors offer a number of advantages over established designs. For example, grid structures for cylindrical detectors are simpler than those for rectangular designs. The goal of our work is to design a cylindrical coplanar grid detector with excellent resolution at low- and high-energy. Information on detector design and manufacturing is presented. Six detectors are characterized. The pulse height resolution of the best detector is 13.5 keV full width at half maximum (FWHM) at 662 keV and 5.5 keV FWHM at 122 keV.

Keywords: CdZnTe, coplanar grid, room temperature, semiconductor, gamma ray detectors, spectroscopy, safeguards

1. INTRODUCTION

A variety of applications require compact and efficient room-temperature semiconductor detectors for gamma-ray spectroscopy. For example, reactor spent fuel measurements for nuclear material safeguards require compact probes with excellent energy resolution and peak shape at high energy (up to 2 MeV). Nuclear material safeguards applications require detectors capable of resolving the low-energy gamma-rays (e.g. the 186 keV gamma-ray from ^{235}U) and intermediate-energy gamma-rays (e.g. the 413.7 keV gamma-ray from ^{239}Pu). To meet these challenges, gamma-ray detectors must have low electronic noise and good peak shape over a wide energy range.

Cylindrical detectors are desired for these applications because their response is independent of orientation and they yield more compact probes than equivalent-volume rectangular detectors. Among the competing electrode designs for single-carrier devices, coplanar grid CdZnTe detectors yield the best charge measurement uniformity and, thus, the best resolution and peak shape for gamma rays above 100 keV. In principle, cylindrical coplanar grid detectors have a number of advantages over rectangular designs in that edge-compensation and electrode interconnection schemes are simpler and sharp corners that could enhance surface leakage are eliminated. The design of cylindrical geometry coplanar grid detectors is simplified by the fact that cylindrical devices are effectively one-dimensional.

To determine the feasibility of cylindrical coplanar grid detectors, we designed and tested detectors suitable for nuclear material attribute measurements. Cylindrical coplanar grid patterns for a 10-mm diameter by 5-mm thick detector were designed by Los Alamos National Laboratory (LANL) using a semiconductor modeling code. The final grid design included edge-compensation and a simple bus-bar interconnection scheme to minimize bond-wire connections. A coarse grid pattern was selected to minimize noise, thus ensuring good low-energy performance. Cylindrical detectors with this pattern were manufactured by eV Products and delivered to LANL for testing. All of the detectors produced outstanding performance at low and high energy. The resolution of the best detector was 13.5 keV FWHM at 662 keV and 5.5 keV FWHM at 122 keV. In this paper, details of the design, manufacture and characterization of these detectors are presented.

[*] Correspondence: Email: thp@lanl.gov; www: http://www.nis5.lanl.gov/; Telephone: 505 667-6449; Fax: 505 665-5910.

2. ELECTRODE DESIGN

Coplanar grid detectors use a subtractive method to compensate for tailing due to hole trapping.[1] The anode electrodes take the form of interdigitated grids that are connected to separate charge-sensitive preamplifiers (Fig. 1a). An electric field is established in the detector bulk by applying bias to the cathode, which is a full-area contact located on the side opposite the grid electrodes. The two grid preamplifiers are connected to a subtraction circuit to produce a difference signal. Bias is applied between the grid electrodes so that one of the grids preferentially collects charge. Charge motion within the detector is sensed equally by the grid electrodes (Fig. 1b). Consequently, the difference signal is insensitive to charge motion within the bulk of the detector. When charge approaches the anode, the grid signals begin to differ and a signal is registered at the output of the difference circuit. In a well-designed detector and in the absence of electron trapping, the magnitude of the difference signal is the same no matter where the charge is generated in the device. This results in a large improvement in performance for gamma-ray spectroscopy when compared to conventional planar device technology (Fig. 1c).

The trapping length for electrons in CdZnTe is on the order of 5 cm under nominal operating conditions (~1000 V/cm). For thick devices (>0.5 cm), the variation in electron trapping as a function of depth in the detector can degrade resolution and peak shape. A simple scheme using analog electronics is routinely employed to compensate for electron trapping. The output signal of one of the preamplifiers is attenuated (e.g. the gain of the noncollecting preamplifier is reduced relative to the collecting preamplifier). This has the effect of flattening out magnitude of the difference signal with depth. This analog technique has been demonstrated to work for devices up to 15 mm thick. It is worth noting that other methods to compensate for electron trapping have been developed.[2] However, to minimize the complexity of the front-end electronics, a simple gain adjustment was used to compensate for electron trapping in the cylindrical detectors described in this paper.

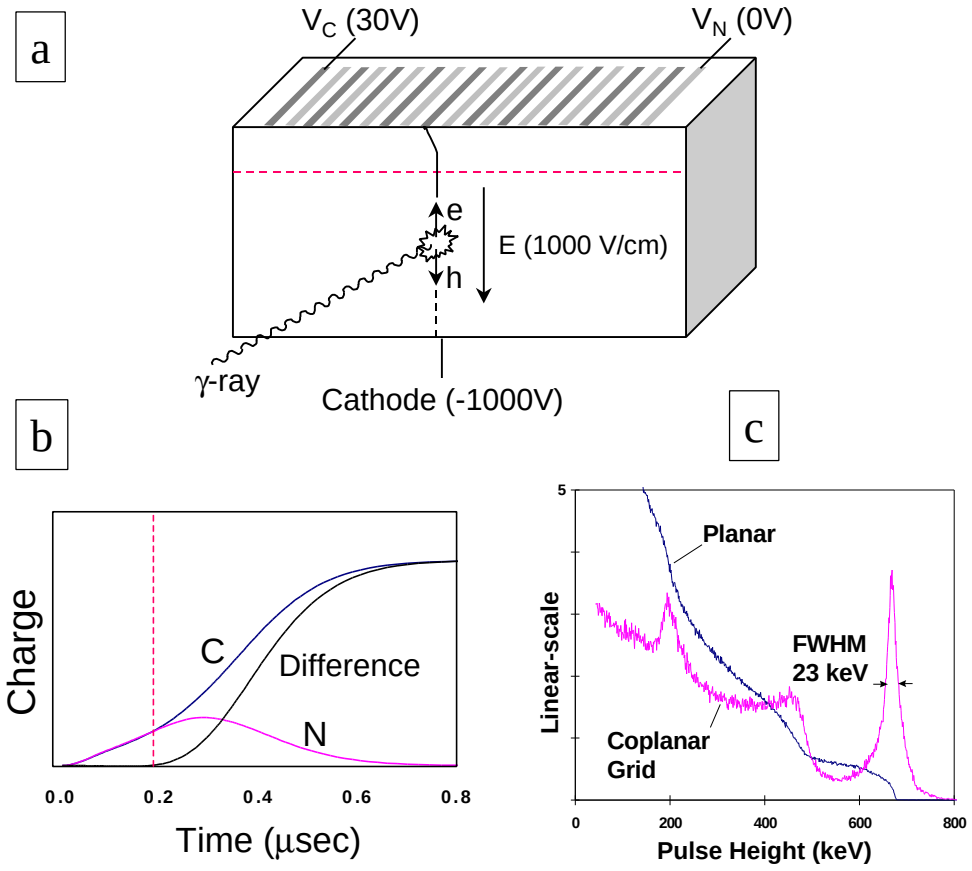

Figure 1. This illustration of coplanar grid technology includes the following: a) Coplanar grid detector geometry and nomenclature (C and N refer to the collecting and noncollecting coplanar grid electrodes, respectively). b) Charge pulse on the collecting, noncollecting, and difference electrodes. c) Comparison between pulse height spectra for the same device (10 mm × 10 mm × 5 mm) operated as a planar detector and as a coplanar grid detector.

There are two competing design criteria for coplanar grid detectors: 1) minimize noise caused by inter-grid leakage current; 2) and maximize the spatial uniformity of charge measurements. Fine grid structures yield uniform charge measurements and, consequently, excellent peak shape for high-energy gamma rays. However, because bias is placed across electrodes that are closely spaced, the use of fine grid structures can lead to high leakage current, resulting in high noise and poor resolution at low energy. Most applications for coplanar grid detectors require better resolution than NaI(Tl) at both low and high energy. For example, in nuclear material safeguards, portable detectors are required that can measure the 186 keV gamma ray from ^{235}U and the 413.7 keV gamma ray from ^{239}Pu. For early commercial coplanar grid detectors, the pulse height resolution at 186 keV was often no better than NaI(Tl) because very fine grid structures were used (<100 μm electrodes and gaps). This was in part due to the lack of a standard for the characterization of coplanar grid detectors. At the time detector developers focused on achieving the best possible pulse height resolution at 662 keV.

For the design of cylindrical detectors, we constrained ourselves to inter-electrode gap sizes greater than 200 μm. Based on experience with coplanar grid detectors manufactured by eV Products, selection of gap sizes greater than 200 μm guaranteed very low inter-electrode leakage. Note that the optimal gap size is somewhat dependent on surface processing technology. New surface processing techniques are being investigated that may lead to finer grid structures with acceptable low-energy performance.[3] We also chose to use a guard ring with our design. Because manufacturing processes for large cylindrical parts had not been perfected, we anticipated the possibility of problems with noise induced by leakage between the cathode and the grid electrodes. The guard ring was included as a contingency to minimize noise cause by leakage across the sides of the detector.

The target size for the detectors was 10 mm in diameter by 5 mm thick (A=0.79 cm^2, V=0.39 cm^3). This size was selected because there was a high probability that a large number of parts could be manufactured with uniform electronic properties and with minimal internal defects (e.g. grain boundaries). This would enable us to focus more on detector design rather than material selection and processing. Detectors of this size were also well matched to specific applications, namely nuclear material attribute measurements and spent fuel analysis.

Uniform charge measurements were achieved using design principles found in the literature.[4,5] The charge (Q) induced on electrodes by the motion of a carrier with charge q within the detector is given by Ramo's theorem,[6] which can be expressed as

$$\frac{dQ}{dt} = q\ \mathbf{v}\cdot\nabla j_w \qquad (1)$$

where $\mathbf{v}$ is the velocity of the carrier and j_w is a function known as the "weighting potential." The weighting potential is determined for a selected set of electrodes by solving Laplace's equation, $\nabla\left(e\nabla j_w\right)=0$, with the electrodes of interest set to unit potential and with all other electrodes grounded. To create a region within the detector in which the difference signal is insensitive to charge motion, the weighting potential for the two grids must match closely over the region. A reasonable strategy for coplanar grid detector design is to design the grid electrodes such that the insensitive region is as large as possible.

With this strategy in mind, we investigated several electrode configurations for cylindrical detectors. All of the structures were cylindrically symmetric. For each configuration, we computed the weighting potential using a finite-elements code capable of modeling cylindrical structures. Results for a design with uniform electrodes and gaps are shown in Fig. 2. The radial electrode structure is shown at the bottom of the figure. Note that the grid electrodes are labeled A and B: Either grid can function as the collecting electrode. Each grid contained 5 electrodes. The width of the gaps and electrodes was 240 microns. The width of the guard ring was 320 microns. The radial variation of the weighting potential for each grid is shown at four different depths below the anode. Note that the weighting potential for grid A was scaled by a factor of 1.2 prior to display in Fig. 2. Even after scaling, the radial variation of the weighting potential for grid A differs significantly from that of grid B. Although this pattern would probably produce functioning coplanar grid detectors, it would probably yield poor pulse height resolution and tailing relative to established rectangular grid designs.

To improve the match between the A- and B-grids, we adjusted the thickness of the electrodes in grid-A at the center and near the edge of the detector. The best trial pattern is presented in Fig. 3. Note that the central electrode and the outermost

electrode for grid-A are twice the width of the other electrodes. The width of the gap and all but the inner and outer electrodes for grid-A was 225 microns. The guard ring was 275 microns. No scaling was used in the comparison between the weighting potential for grids A and B. Note that there is a considerable improvement over the uniform grid in terms of consistency between the weighting potential for grids A and B. Below a depth of 2 cm, the root-mean-square (RMS) difference between the weighting potential for the A- and B-grids was 2.3%. The uniform grid structure was found to have an RMS difference of 5.9% below 2 cm. The grid structure shown in Fig. 3 was used to pattern detectors used in this study.

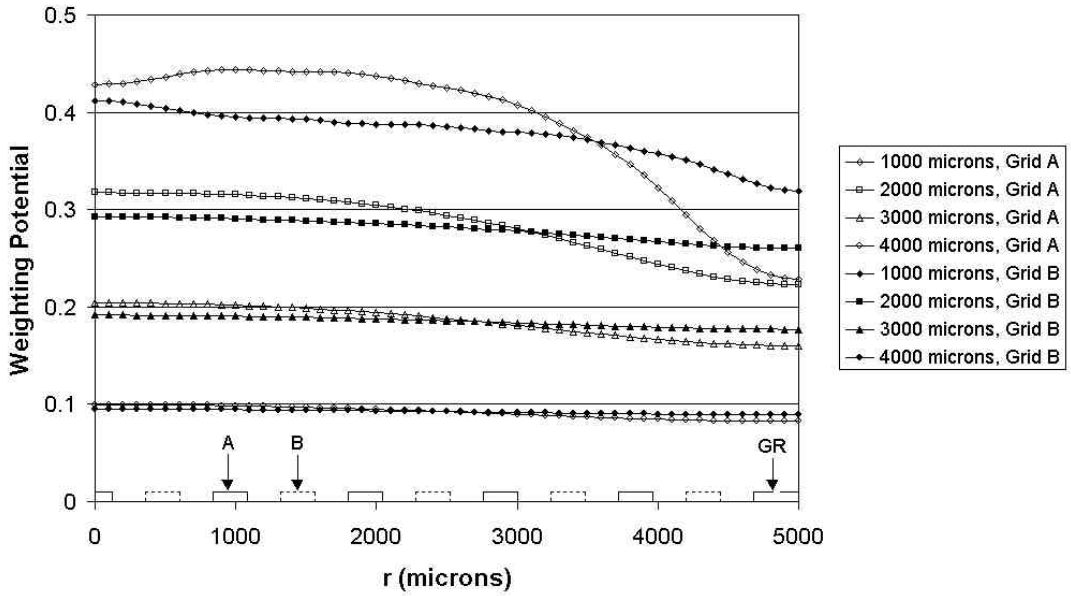

Figure 2. Weighting potential for a uniform grid pattern (with guard ring). The radial electrode pattern is shown. The coplanar grid electrodes are labeled A and B. The guard ring is labeled GR.

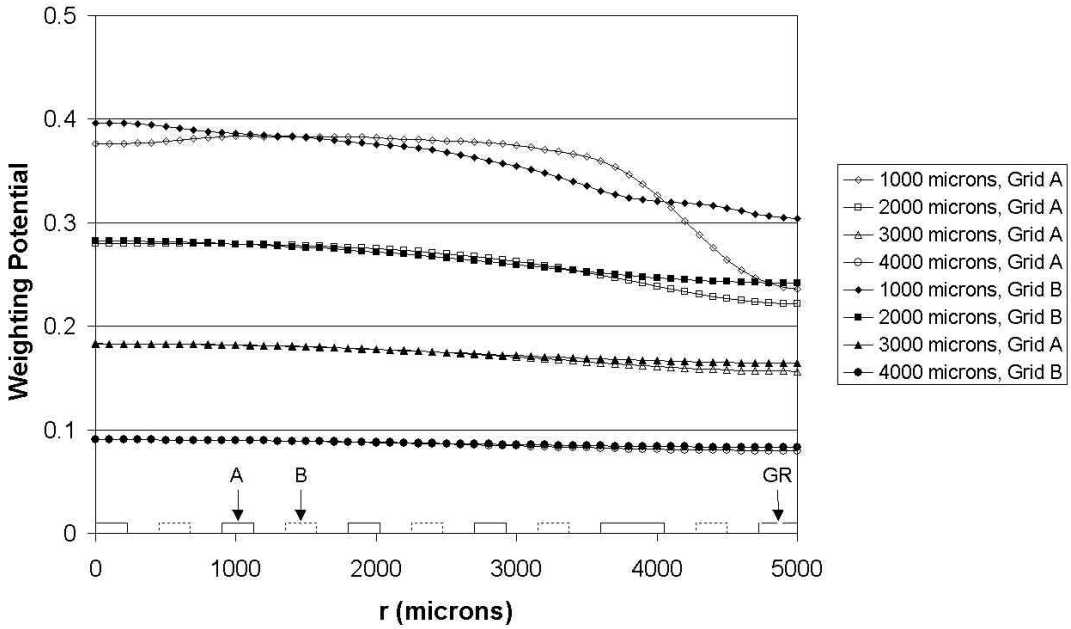

Figure 3. Weighting potential for a modified grid pattern (with guard ring). The radial electrode pattern is shown. The coplanar grid electrodes are labeled A and B. The guard ring is labeled GR.

3. MANUFACTURING

Material from two ingots (I03 and C26) was used to manufacture cylindrical parts. Axial slices were taken from each ingot. Square blanks were cut from regions of the slices determined to be free of grain boundaries (by visual inspection) and internal defects (by infrared inspection). Then, a lathe was used to round off the corners of the parts to produce cylinders. The final parts were 10 mm in diameter by 5 mm thick. A total of 30 parts were manufactured. Since no technique was available to polish the curved sides of the detectors, the cylindrical parts were etched in Bromine Methanol to relieve surface damage. The flat faces of the parts were polished to enable patterning. Lift-off photolithography followed by sputtering was used to deposit electrodes on the surface. The electrodes consisted of a thin platinum deposit followed by a thicker gold deposit for bond-wire connection.

Connecting bond wires to individual electrodes is tedious. Consequently, commercial coplanar grid detectors are equipped with bus bars to interconnect the grids. By interconnecting the grids on the surface, the effort required to make electrical connection is reduced along with the likelihood of a wire disconnecting from an electrode during the lifetime of the detector. We developed a bus-bar interconnection scheme for cylindrical coplanar grid detectors. Electrode patterns for cylindrical coplanar grid detectors are shown in Fig. 4. Pattern 1 requires wire bonding to each electrode. Patterns 2, 3, and 4 have an interconnecting bus bar. For these patterns, connections are required only for the two grids and the guard ring. The design is intended to provide electrical interconnection with minimal distortion to the weighting potential. At the time, the minimum feature size that could be produced reliably by photolithography was 50 μm. To investigate the effect of bus-bar width on the performance of the detector, we varied bus-bar parameters: Pattern 2 has a 50 μm bus-bar that is separated from the other electrodes by a 100 μm gap; Pattern 3 has a 100 μm bus-bar with a 150 μm gap; Pattern 4 has a 100 μm bus-bar with a 200 μm gap.

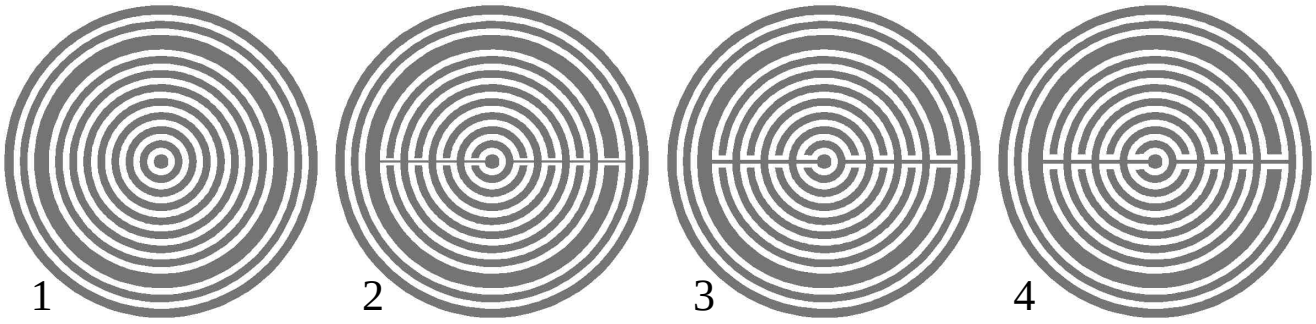

Figure 4. Grid patterns applied to cylindrical parts using photolithography: 1) No bus bar; 2) 50 μm bus bar with 100 μm gaps; 3) 100 μm bus bar with 150 μm gaps; 4) 100 μm bus bar with 200 μm gaps.

Following patterning, the parts were tested in a probe station. All of the parts tested held high voltage (>500V) and produced peaks when operated in coplanar grid mode. Parts that performed well in the probe station were mounted on an alumina substrate. Bonding wire was used to connect the grid electrodes and guard ring to posts with sockets for connection to front-end pulse shaping electronics. A complete detector element is shown in Fig. 5. As a final step, most of the detectors were coated with a protective paint that also served to reduce surface leakage current.

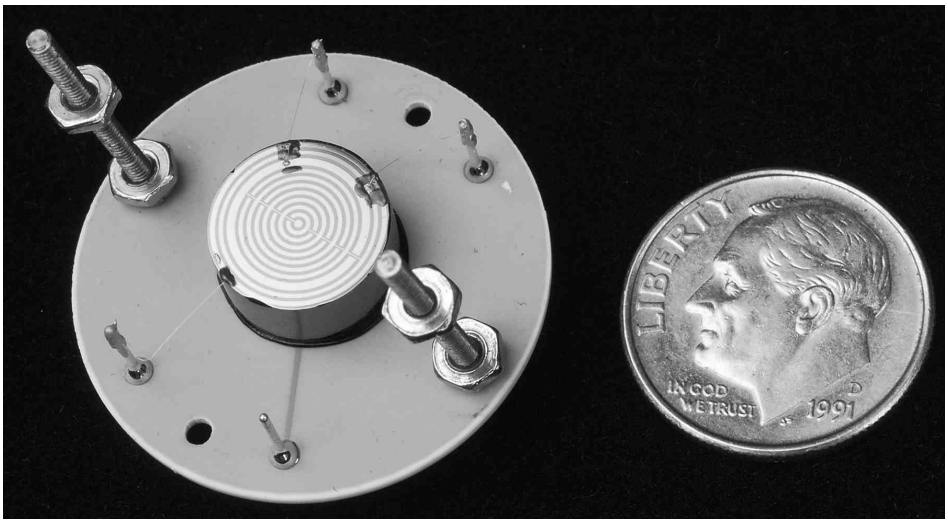

Figure 5. Detector I03-06 mounted on a ceramic substrate.

4. CHARACTERIZATION

Six of the detectors were characterized in detail. Optimal settings were found for each detector. The performance of the detectors for gamma-ray spectroscopy was evaluated. Noise characteristics, I-V curves, and counting efficiency were also measured. Noise measurements were made under optimal operating conditions using a pulser and are shown in Fig. 6. From the standpoint of noise, the optimal amplifier shaping time is ~0.5 μs. This setting was also found to yield the best pulse height resolution at 662 keV and was used in all of the measurements of pulse-height spectra presented in this paper.

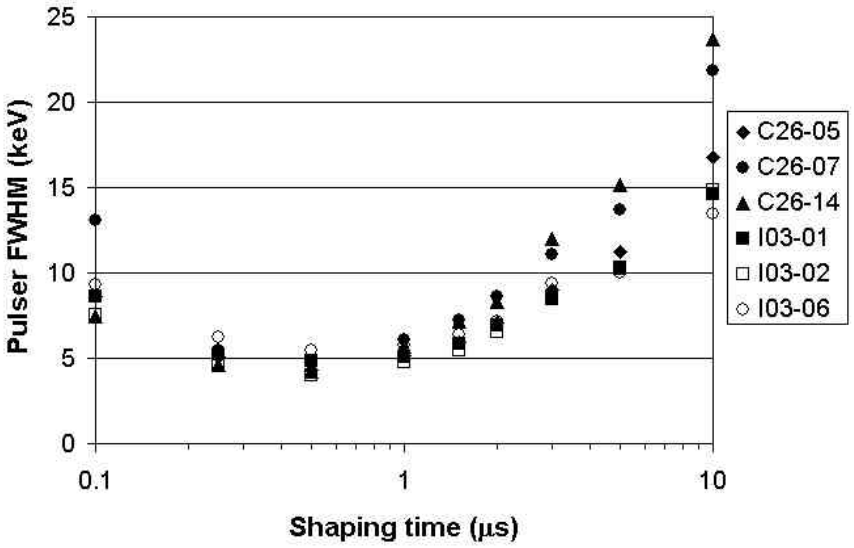

Figure 6. Pulser FWHM as a function of amplifier shaping time.

Coplanar grid detectors have three settings that can be adjusted (differential bias, bulk bias, and the gain on the difference circuit). In addition, there are four different configurations for coplanar grid detectors, achieved by switching the grid lead wires and reversing the polarity of the differential bias. All configurations were tested with a range of settings to determine optimal operating conditions. Note that the optimization was carried out with the primary goal of achieving the best possible pulse-height resolution at 662 keV. However, at each step of the optimization, the detectors were placed in a well-defined geometry and counting efficiency was recorded. Results of the optimization are presented in Table 1. Relative efficiency values were obtained using a fixed counting geometry. The quoted values are for full-energy efficiency (also known as

photo-peak efficiency). Peak areas used to estimate full energy efficiency were obtained using standard region-of-interest methods. Pulse-height spectra ^{137}Cs (662 keV) and ^{57}Co (122 keV and 136 keV) taken with the optimal settings are displayed in Fig. 7.

Table 1. Detector settings and performance under optimal conditions.

Detector	Grid Pattern	Bulk Bias (V)	Grid Bias (V)	FWHM at 122 keV (keV)	Relative Efficiency at 122 keV	FWHM at 662 keV (keV)	Relative Efficiency at 662 keV
C26-05	3	-1500	-99	6.3	0.87	12.5	0.66
C26-07	4	-1500	-99	7.2	0.82	18.9	0.66
C26-14	1	-1000	-99	8.1	0.67	16.2	0.66
I03-01	1	-1000	-28	7.1	0.88	14.0	0.79
I03-02	1	-800	-32	6.7	1.00	13.4	1.00
I03-06	2	-1200	-28	4.3	0.79	15.6	0.91

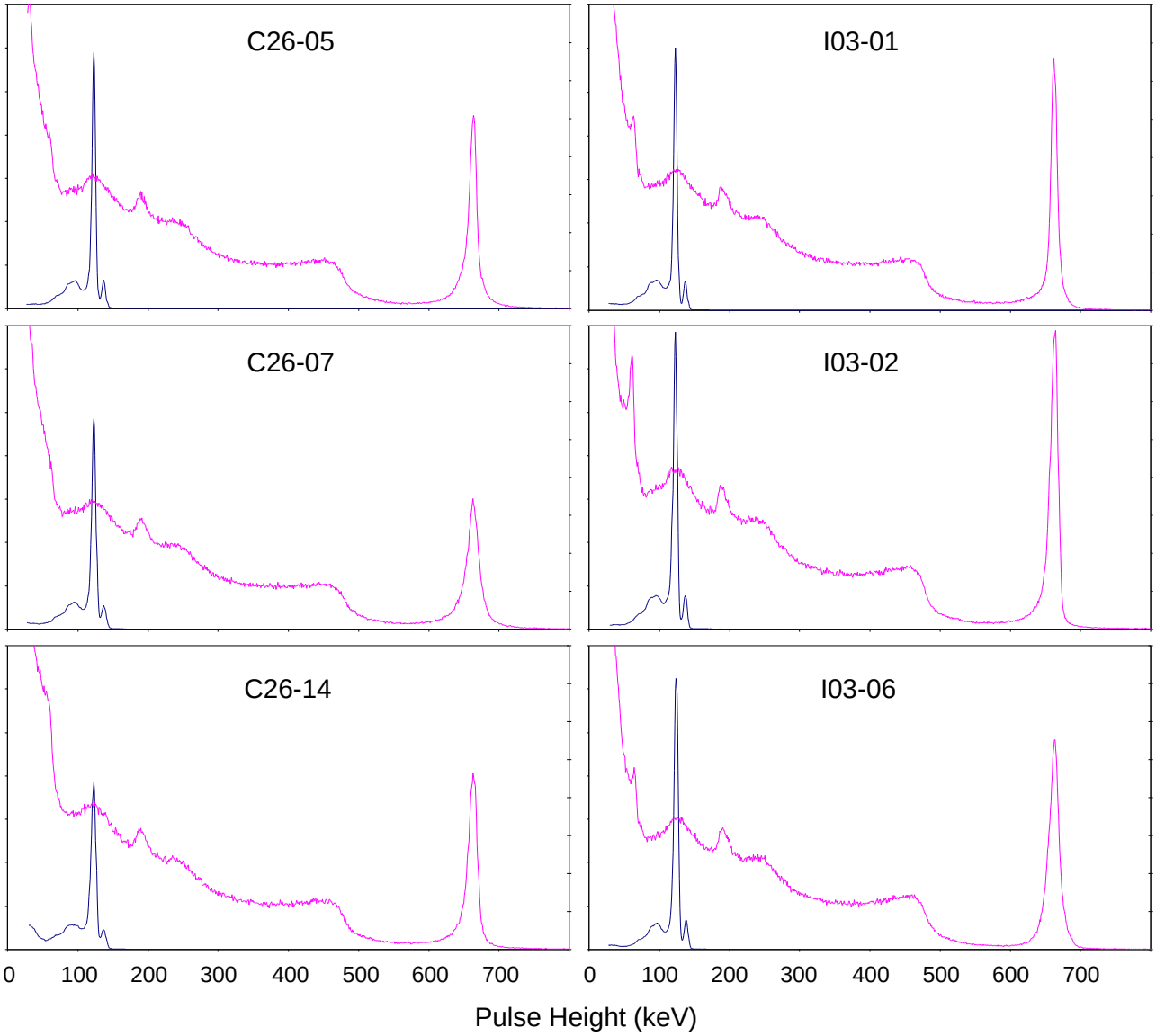

Figure 7. Pulse height spectra for all six detectors.

5. DISCUSSION

Considerable variation was observed in the full energy efficiency for the six detectors tested. Detectors manufactured from the C26 ingot had significantly lower full energy efficiency at 662 keV than detectors manufactured from I03. C26 detectors also achieved the best performance at higher differential bias values than the I03 detectors. This is probably due to differences in material properties between the two ingots, rather than macroscopic defects in the crystal (e.g. grain boundaries). It was also noted during the characterization that the optimal resolution settings did not always correspond to the highest detection efficiency. Gains in efficiency can be made using non-optimal resolution settings with relatively minor losses in resolution.

The absolute full energy efficiency of the detectors was determined by measuring a ^{137}Cs source with known activity in a well-defined geometry. Our goal was to compare the efficiency of our detectors relative to an ideal detector with 10-mm diameter by 5-mm thick active volume. We used a Monte Carlo radiation transport code to calculate the full energy efficiency of the ideal detector (assuming 10% zinc) and compared the calculated efficiency to the experimental result. We estimate that I03-02, the most efficient detector, was between 80% and 90% the efficiency of an ideal detector of the same size. Note that there are several factors that could influence this result, including charge loss due to electron transport, which was not modeled. There are several reasons why detectors would have less than 100% volume utilization for the full energy efficiency measurement, including: the presence of bulk defects that trap electrons such as grain boundaries; variations in the weighting potential near the anode; parasitic collection of electrons by noncollecting electrodes. These issues will be investigated in future work.

The use of a bus bar for grid interconnection did not significantly degrade pulse height resolution either at low or high energy. One of the best detectors (I03-06) used a 50-micron bus bar with 100-micron gaps. However, C26-07, which produced the worst resolution at 662 keV, used thick bus bars and gaps (100 microns and 200 microns, respectively). The relatively poor performance of this detector may be caused by distortions in the weighting field near the center of the device. Because the design with thin bus bars and gaps functioned effectively, it will be used in future detectors.

6. CONCLUSIONS

We have developed the first cylindrical coplanar grid CdZnTe detectors. Use of cylindrical geometry greatly simplifies electrode design in that one-dimensional coplanar structures can be generated. A finite element code was used to optimize cylindrical electrode patterns and manufacturing processes were developed to machine cylindrical parts. The grid design was developed to balance pulse height resolution at low and high gamma ray energy. A bus bar interconnect scheme was developed to minimize the effort required to connect bond wires to the grid electrodes. Six detectors were patterned and tested. All six of the detectors meet resolution requirements for the target application: nuclear material attribute measurements. The pulse height resolution of the best detector is 13.5 keV full width at half maximum (FWHM) at 662 keV and 5.5 keV FWHM at 122 keV. The resolution achieved at 662 keV (~2% FWHM) is comparable to that achieved by well-optimized rectangular grid designs for detectors with similar size. The resolution achieved at 122 keV (~4-keV to 8-keV) is significantly better than NaI(Tl) and is an improvement over earlier coplanar grid designs. Lessons learned from this exercise will be used to further optimize cylindrical coplanar grid detectors for different applications.

ACKNOWLEDGEMENTS

This work was funded by Laboratory Directed Research and Development through the Department of Energy under contract W-7405-ENG-36.

REFERENCES

1. Luke, P. N., "Single-polarity charge sensing in ionization detectors using coplanar electrodes," Applied Physics Letters v. 65(#22) pp. 2884-2886 (1994).
2. He, Z., G. F. Knoll, D. K. Wehe, et al., "Position-sensitive single carrier CdZnTe detectors," Nuclear Instruments and Methods in Physics Research A, v. 388 pp. 180-185 (1997).
3. Prettyman, T. H., M. A. Hoffbauer, J. A. Rennie, et al., "Performance of CdZnTe detectors passivated with energetic oxygen atoms," Nuclear Instruments and Methods in Physics Research A, v. 422(#1-3) pp. 179-184 (1999).
4. Luke, P. N., M. Amman, T. H. Prettyman, et al., "Electrode Design for Coplanar-Grid Detectors," IEEE Transactions on Nuclear Science, v. 44(#3/pt.1) pp. 713-720 (1997).
5. He, Z., G. F. Knoll, D. K. Wehe, et al., "Coplanar grid patterns and their effect on energy resolution of CdZnTe detectors," Nuclear Instruments and Methods in Physics Research A, v. 411 pp. 107-113 (1998).
6. Ramo, S., "Currents induced by electron motion," Proc. IRE v. 27 p. 584 (1939).